

# EQUILIBRIUM THEORY OF AN INTENSE ELLIPTIC BEAM FOR HIGH-POWER RIBBON-BEAM KLYSTRON APPLICATIONS\*

C. Chen and J. Zhou, MIT Plasma Science and Fusion Center, Cambridge, MA 02139, USA

## Abstract

Realization of the concept for a high-power ribbon-beam klystron (RBK) requires a novel large-aspect ratio elliptic electron beam instead of a conventional circular electron beam. In this paper, a cold-fluid equilibrium theory of a nearly non-twisting intense elliptic charged-particle beam is presented. The equilibrium theory is applied in designs of elliptic electron beams for high-power RBKs. Results of the design and simulation of a 20:1 elliptic electron beam for a 10 MW, 1.3 GHz International Linear Collider (ILC) RBK are discussed.

## INTRODUCTION

A major thrust in the International Linear Collider (ILC) program is the development of high-power klystrons to power a TeV-class LC. The high construction and operating costs of the ILC rf power system drive the need for research and development on Alternative Configuration Design (ACD).

For ILC, the choice of Base Configuration Design (BCD) is the L-Band Multi-Beam Klystron (MBK). The required specifications for the L-Band power source are: 10 MW power output, 1.5 ms pulse length, 10 Hz repetition rate, 65% efficiency, and several years of lifetime.

Much progress has been made in Europe, US and Japan on L-Band MBK. At Thales, 4 tubes were produced, and gun arcing problem occurred and seemed to be corrected in last two tubes after fixes applied. However, Thales tubes recently developed other arcing problems above 8 MW. Thales is to build two more without changes and two with changes after problem is better diagnosed. At CPI, one tube was built and factory-tested to 10 MW at short pulse. During full pulse testing at DESY, it developed vacuum leak after 8.3 MW was achieved. It has been repaired and will be tested again. At Toshiba, one tube was built, and after a vacuum problem was fixed, ran at full spec for one day – has been shipped to DESY for further evaluation. Despite these efforts, the ILC community and industry still needs to develop an L-Band klystron that meets the full specifications for ILC.

A leading choice of Alternative Configuration Design (ACD) is a ribbon-beam (or sheet-beam) klystron (RBK) powered by an electron beam with a large-aspect-ratio elliptic cross section. The ribbon-beam klystron (RBK) has the following advantages over the conventional multiple cylindrical-beam klystrons:

- Higher efficiency (75% vs. 65%),
- Single beam (1 vs. 6 or 7),

- Energy-free permanent magnet vs. energy-consuming pulsed magnet.

These advantages would reduce the construction and operating costs of ILC and improve the reliability of the rf power system. RBKs could provide the following savings:

- Klystron hardware: 66% (or \$60M) saving.
- RF system electricity: 20% (or \$20M/year) saving.

These advantages and cost savings motivated us to pursue the R&D on a RBK at Massachusetts Institute Technology. The goal of MIT R&D program is to continue our innovative research on ribbon-beam klystrons, building upon the experience we gained in the past several years in the theory, design, fabrication, and testing of ribbon beams and ribbon-beam devices.

The purposes of this paper are to present a cold-fluid equilibrium theory of a nearly non-twisting intense elliptic charged-particle beam, and to apply it in the design of a 20:1 elliptic electron beam for the development of the ILC RBA.

## COLD-FLUID EQUILIBRIUM THEORY OF A NEARLY NONTWISTING ELLIPTIC CHARGED-PARTICLE BEAM

We have developed both cold-fluid and kinetic equilibrium theories of nearly non-twisting intense elliptic charged-particle beams. While the kinetic theory has been presented elsewhere [1], this paper discusses the cold-fluid theory. In the paraxial approximation, the focusing field is expressed as

$$\mathbf{B}^{ext} = -B_0 \sin(k_0 s) \mathbf{e}_z + B_0 \cos(k_0 s) \times \left( \frac{k_{0x}^2}{k_0} x \mathbf{e}_x + \frac{k_{0y}^2}{k_0} y \mathbf{e}_y \right) + B'_q (y \mathbf{e}_x + x \mathbf{e}_y) \quad (1)$$

with  $B'_q \equiv \partial B_x^q / \partial y|_{(s,0,0)} = \partial B_y^q / \partial x|_{(s,0,0)}$  and  $k_{0x}^2 + k_{0y}^2 = k_0^2 \equiv (2\pi/S)^2$ . The paraxial cold-fluid equations consist of the continuity equation, the Poisson equation, and the force balance equation, i.e.,

$$\beta_b c \frac{\partial}{\partial s} n_b + \nabla_{\perp} \cdot (n_b \mathbf{V}_{\perp}) = 0, \quad (2)$$

$$\nabla_{\perp}^2 \phi^s = \beta_b^{-1} \nabla_{\perp}^2 A_z^s = -4\pi q n_b, \quad (3)$$

$$n_b \left( \beta_b c \frac{\partial}{\partial s} + \mathbf{V}_{\perp} \cdot \nabla_{\perp} \right) \mathbf{V}_{\perp} = \frac{q n_b}{\gamma_b m} \left[ -\frac{1}{\gamma_b^2} \nabla_{\perp} \phi^s + \beta_b \hat{\mathbf{e}}_z \times \mathbf{B}_{\perp}^{ext} + \frac{\mathbf{V}_{\perp}}{c} \times B_z^{ext}(s) \hat{\mathbf{e}}_z \right], \quad (4)$$

\*Research supported by US Department of Energy, Office of High-Energy Physics, Grant No. DE-FG02-95ER40919 and Air Force Office of Scientific Research, Grant No. FA9550-06-1-0269.

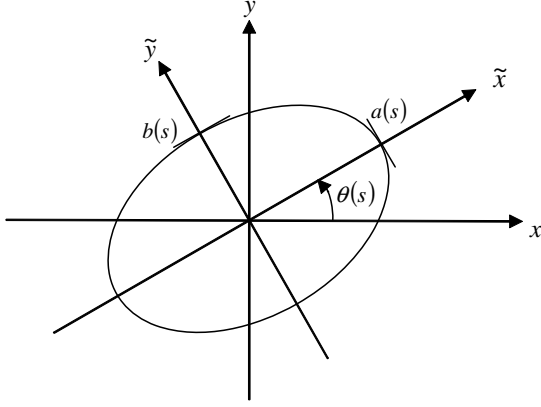


Figure 1: Coordinate systems.

where  $s = z$ ,  $\mathbf{x}_\perp = x\hat{\mathbf{e}}_x + y\hat{\mathbf{e}}_y$ ,  $\nabla_\perp = \partial/\partial\mathbf{x}_\perp$ ,  $q$  and  $m$  are the particle charge and rest mass, respectively,  $n_b$  is the particle density,  $\mathbf{V}_\perp$  is the transverse flow velocity,  $\gamma_b = (1 - \beta_b^2)^{-1/2}$  is the relativistic mass factor, use has been made of  $\beta_z = V_z/c \equiv \beta_b = \text{const}$ ,  $c$  is the speed of light in vacuum, and the self-electric field  $\mathbf{E}^s$  and self-magnetic field  $\mathbf{B}^s$  are determined from the scalar potential  $\phi^s$  and vector potential  $A_z^s\hat{\mathbf{e}}_z$ , i.e.,  $\mathbf{E}^s = -\nabla_\perp\phi^s$  and  $\mathbf{B}^s = \nabla_\perp \times A_z^s\hat{\mathbf{e}}_z$ .

Equation (2)-(4) are solved with the density and transverse velocity of the form

$$n_b(\mathbf{x}_\perp, s) = \frac{N_b}{\pi a(s)b(s)} \Theta \left[ 1 - \frac{\tilde{x}^2}{a^2(s)} - \frac{\tilde{y}^2}{b^2(s)} \right], \quad (5)$$

$$\mathbf{V}_\perp(\mathbf{x}_\perp, s) = [\mu_x(s)\tilde{x} - \alpha_x(s)\tilde{y}] \beta_b c \hat{\mathbf{e}}_{\tilde{x}} + [\mu_y(s)\tilde{y} + \alpha_y(s)\tilde{x}] \beta_b c \hat{\mathbf{e}}_{\tilde{y}}. \quad (6)$$

In Eqs. (5) and (6),  $\mathbf{x}_\perp = \tilde{x}\hat{\mathbf{e}}_{\tilde{x}} + \tilde{y}\hat{\mathbf{e}}_{\tilde{y}}$  is a transverse displacement in the twisted coordinate system illustrated in Fig. 1.  $\theta(s)$  is the twist angle of the ellipse.  $\Theta(x) = 1$  if  $x > 0$  and  $\Theta(x) = 0$  if  $x < 0$ . The functions  $a(s)$ ,  $b(s)$ ,  $\mu_x(s) = a^{-1}da/ds$ ,  $\mu_y(s) = b^{-1}db/ds$ ,  $\alpha_x(s)$ ,  $\alpha_y(s)$  and  $\theta(s)$  obey the generalized envelope equations

$$\begin{aligned} & \frac{d^2 a}{ds^2} - \frac{b^2(\alpha_x^2 - 2\alpha_x\alpha_y) + a^2\alpha_y}{a^2 - b^2} a \\ & - \frac{2K}{(a+b)} + 2\sqrt{\kappa_0}\alpha_y B_0 \sin(k_0 s)a - 2\sqrt{\kappa_0} \\ & \times \left[ \frac{k_{0x}^2 - k_{0y}^2}{2k_0} B_0 \cos(k_0 s) \sin 2\theta - B'_q \cos 2\theta \right] a = 0 \end{aligned} \quad (7)$$

$$\begin{aligned} & \frac{d^2 b}{ds^2} + \frac{a^2(\alpha_y^2 - 2\alpha_x\alpha_y) + b^2\alpha_x}{a^2 - b^2} b \\ & - \frac{2K}{(a+b)} + 2\sqrt{\kappa_0}\alpha_x B_0 \sin(k_0 s)b + 2\sqrt{\kappa_0} \\ & \times \left[ \frac{k_{0x}^2 - k_{0y}^2}{2k_0} B_0 \cos(k_0 s) \sin 2\theta - B'_q \cos 2\theta \right] b = 0 \end{aligned} \quad (8)$$

$$\begin{aligned} & \frac{d}{ds} (a^2\alpha_x) - \frac{ab^3(\alpha_x - \alpha_y)}{a^2 - b^2} \frac{d}{ds} \left( \frac{a}{b} \right) \\ & - 2a'a\sqrt{\kappa_0} B_0 \sin(k_0 s) - 2\sqrt{\kappa_0} a^2 \\ & \times \left[ \frac{k_{0x}^2 \cos^2 2\theta + k_{0y}^2 \sin^2 2\theta}{2k_0} B_0 \cos(k_0 s) + B'_q \sin 2\theta \right] = 0 \end{aligned} \quad (9)$$

$$\begin{aligned} & \frac{d}{ds} (b^2\alpha_y) - \frac{a^3b(\alpha_x - \alpha_y)}{a^2 - b^2} \frac{d}{ds} \left( \frac{b}{a} \right) \\ & - 2b'b\sqrt{\kappa_0} B_0 \sin(k_0 s) - 2\sqrt{\kappa_0} b^2 \\ & \times \left[ \frac{k_{0x}^2 \sin^2 2\theta + k_{0y}^2 \cos^2 2\theta}{2k_0} B_0 \cos(k_0 s) + B'_q \sin 2\theta \right] = 0 \end{aligned} \quad (10)$$

$$\frac{d\theta}{ds} = \frac{a^2\alpha_y - b^2\alpha_x}{a^2 - b^2}, \quad (11)$$

where  $K \equiv 2q^2 N_b / \gamma_b^3 \beta_b^2 m c^2$ ,  $\sqrt{\kappa_0} = q / 2\gamma_b \beta_b m c^2$ , and Equations (5)-(6) together with the generalized envelope equations (7)-(11) provide a theoretical framework for the design of nearly non-twisting intense elliptic charged-particle beams.

Without the magnetic quadrupole, the beam ellipse will exhibit noticeable periodic twists as the beam propagates through the focusing channel, as shown previously [3, 4]. The magnetic quadrupole reduces the amplitude of periodic twists significantly, permitting nearly non-twisting elliptic charged-particle beams.

## DESIGN AND SIMULATION OF AN ELLIPTIC ELECTRON BEAM FOR ILC RBK APPLICATIONS

Using the cold-fluid equilibrium theory presented above, we have determined the parameters for the realization of an elliptic electron beam in an ILC ribbon beam klystron.

Figure 2 shows the results of the two-dimensional particle-in-cell (PIC) simulation using the MIT 2D Periodically Focused Beam (PFB2D) code [3, 4] for the parameters of our consideration of an elliptic beam for the ILC RBK listed in Table 1.

In this design, the ratio of the semi-major axis to the semi-minor axis is 20:1. The period of the focusing field is chosen to be  $S = 2\pi/k_0 = 2.2$  cm. The amplitude of periodic dipole field is  $B_0 = 2.0$  kG, which is realizable with ellipse-shape dipole permanent magnets [5].

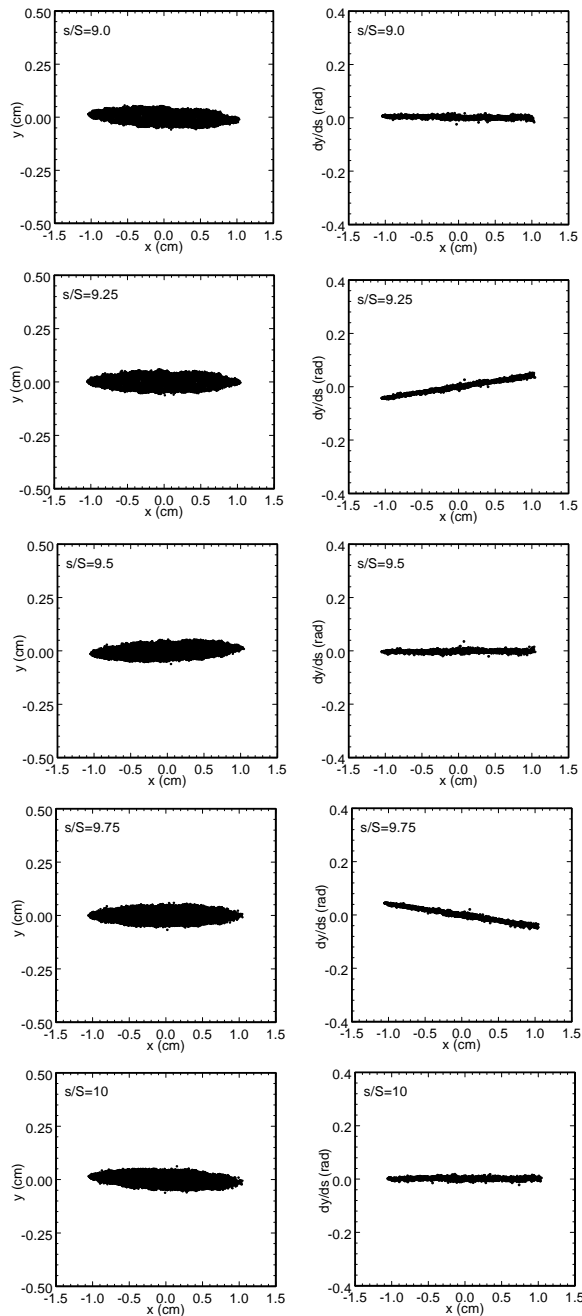


Figure 2: Plots of 5,000 particles (a sample of the  $5 \times 10^5$  particles in the PFB2D simulation) in the  $(x, y)$  plane and  $(x, dy/ds)$  plane for five snapshots within one period:  $s/S = 9.0, 9.25, 9.5, 9.75,$  and  $10$  for the parameters listed in Table 1.

Table 1: System parameters for an elliptic beam design for ILC RBK

Parameter	Value
Current (A)	111.1
Voltage (kV)	120
S (cm)	2.2
$k_{0x}/k_{0y}$	0.158
$B_0$ (kG)	2.0
$B'_q$ (G/cm)	30.4
a/b	20
a (cm)	1.0
$\theta_{\max}$ (deg)	0.75

In the simulation, free-space boundary conditions are used. The beam ellipse is nearly straight with the amplitude of  $0.75^\circ$  in twist angle.

## CONCLUSION

A cold-fluid equilibrium theory of a nearly non-twisting intense elliptic charged-particle beam has been presented. The focusing field consists of a combination of a periodic stack of elliptic dipole magnets and a quadrupole magnet. The theory has been confirmed by two dimensional particle-in-cell simulations using the MIT PFD2D code. It has been applied in the design of a 20:1 elliptic electron beam for the development of the ILC ribbon-beam klystron.

## REFERENCES

- [1] R.J. Bhatt, "Inverse Problems in Intense Elliptic Charged-Particle Beams," Ph.D. Thesis, MIT (2006).
- [2] J. Zhou and C. Chen, "Cold-fluid equilibrium theory of a nearly non-twisting intense elliptic charged-particle beam," manuscript in preparation (2007).
- [3] J. Zhou, "Transport of Intense Elliptic Beams," Ph.D. Thesis, MIT (2006).
- [4] J. Zhou, R. Bhatt and C. Chen, Phys. Rev. ST Accel. Beams **9**, 034401(2006).
- [5] C. Chen, R. Bhatt, A. Radovinsky, J. Zhou, and R. Bhatt, "Three-Dimensional Design of a Non-Asymmetric Periodic Permanent Magnet Focusing System," Proc. 2005 Part. Accel. Conf. (2005), p. 1964.